

# Effect of Atomic Coherence on Absorption in Four-level Atomic Systems: an Analytical Study

S N Sandhya  
Indian Institute of Technology  
KANPUR 208016 INDIA  
email: sns@iitk.ac.in

July 15, 2018

## Abstract

Absorption profile of a four-level ladder atomic system interacting with three driving fields is studied perturbatively and analytical results are presented. Numerical results where the driving field strengths are treated upto all orders are presented. The absorption features is studied in two regimes, i) the weak middle transition coupling, i.e.  $\Omega_2 \ll \Omega_{1,3}$  and ii) the strong middle transition coupling  $\Omega_2 \gg \Omega_{1,3}$ . In case i), it is shown that the ground state absorption and the saturation characteristics of the population of level 2 reveal deviation due to the presence of upper level couplings. In particular, the saturation curve for the population of level 2 shows a dip for  $\Omega_1 = \Omega_3$ . While the populations of levels 3 and 4 show a maxima when this resonance condition is satisfied. Thus the resonance condition provides a criterion for maximally populating the upper levels. A second order perturbation calculation reveals the nature of this minima (maxima). In the second case, I report two important features: a) Filtering of the Autler-Townes doublet in the three-peak absorption profile of the ground state, which is achieved by detuning only the upper most coupling field, and b) control of line-width by controlling the strength of the upper coupling fields. This filtering technique coupled with the control of linewidth could prove to be very useful for high resolution studies.

## 1 Introduction

It is well known that the control of absorption and emission properties of atoms may be achieved by controlling the nature of atomic coherence. Driving field strengths and detunings provide the necessary tuning parameters to achieve this control. Multi-level atoms have the advantage of providing a larger set of tuning parameters. Three level atoms show a class of phenomena which are absorption

inhibitive [1] while four-level systems have shown absorption inducive features at three photon resonance [2]. The narrow absorption features which have been seen in four level systems is attributed to the interaction of double dark resonances [3]. Scully et al [4] report the occurrence of Doppler-free absorption, which has also been reported earlier [2]. Other features which have been reported in four-level systems include coherence switching [5], photon switching (two-photon absorption) [6], fast switching of nonlinear absorption [7], enhancement and suppression of two photon absorption [8] and the occurrence of three peaked absorption [2, 9, 10, 11]. In this paper we investigate the absorption properties and the modification of the ground state absorption due to the additional upper transition couplings. In section II the details of the model is described and the equation of motion is set up. Previous studies [12] have revealed that the dynamics of four-level atoms interacting with three driving fields may be classified into two broad domains, i) the weak middle transition coupling and ii) the strong middle transition coupling. Hence, the analysis is presented separately for these two cases in sections III and IV respectively. In both the cases analytical results are derived perturbatively and the qualitative features are compared with exact numerical calculations which are illustrated graphically.

## 2 Equation of motion.

The model we consider consists of a four-level ladder system shown in Fig 1. The only dipole allowed transitions are  $1 \leftrightarrow 2$ ,  $2 \leftrightarrow 3$ , and  $3 \leftrightarrow 4$  coupled respectively by the Rabi frequencies  $\Omega_1, \Omega_2, \Omega_3$  and the Bohr frequencies are denoted by  $\omega_i, i = 1, 3$ . The decay constants corresponding to the respective levels are denoted by  $\Gamma_i, i=1,4$ . The frequency of the applied fields are denoted by  $\omega_{L_i}, i = 1, 3$  and the detunings are denoted by  $\Delta_i, i = 1, 3$  corresponding to the three couplings. The analysis presented here can also in principle be valid to any other type of 4-level system with transitions such that not more than two dipole transitions share a single level. This could include 'N' type systems as well as the mirror reflected 'N' type systems. This particular ladder system may be identified, for example with the Rb hyper fine levels. For instance, the  $5s_{\frac{1}{2}}, 5p_{\frac{3}{2}}$  and  $5d_{\frac{5}{2}}$  could correspond to the three levels with an additional hyperfine level corresponding to either  $5p_{\frac{3}{2}}$  or  $5d_{\frac{5}{2}}$ . In fact the decay parameters of the model have been chosen to be the same as the decay constants of these levels,  $\Gamma_2 = 6\gamma, \Gamma_3 = \gamma$  and  $\Gamma_4 = \gamma$  in terms of the ground state life time  $\gamma$  which is chosen to be one for convenience. The density matrix equations ([12]) are written in the rotating wave approximation as

$$\begin{aligned} \frac{\partial \rho_{12}}{\partial t} &= (-i\Delta_1 - \Gamma_2/2)\rho_{12} - i\Omega_1(\rho_{22} - \rho_{11}) + i\Omega_2\rho_{13} \\ \frac{\partial \rho_{23}}{\partial t} &= (-i\Delta_2 - (\Gamma_2 + \Gamma_3)/2)\rho_{23} - i\Omega_1\rho_{13} - i\Omega_2(\rho_{33} - \rho_{22}) + i\Omega_3\rho_{24} \end{aligned}$$

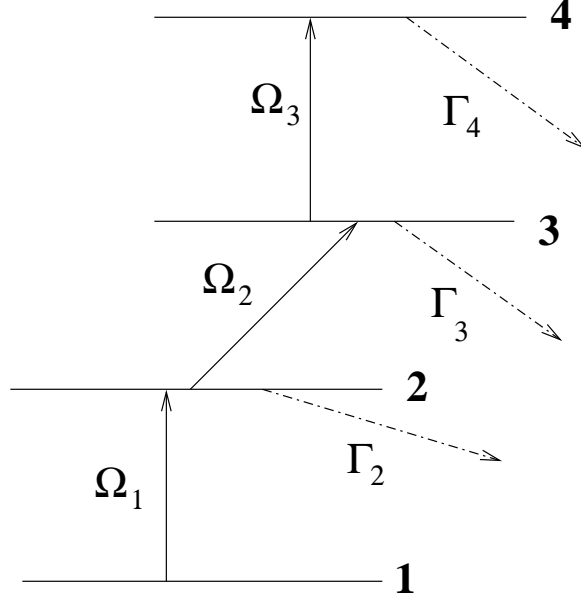


Figure 1: Four-level system interacting with three driving fields of strengths  $\Omega_1, \Omega_2, \Omega_3$ .  $\Gamma_2, \Gamma_3, \Gamma_4$  are the decay constants of the corresponding levels.

$$\begin{aligned}
\frac{\partial \rho_{34}}{\partial t} &= (-i\Delta_3 - (\Gamma_3 + \Gamma_4)/2)\rho_{34} - i\Omega_2\rho_{24} - i\Omega_3(\rho_{44} - \rho_{33}) \\
\frac{\partial \rho_{13}}{\partial t} &= (-i(\Delta_1 + \Delta_2) - \Gamma_3/2)\rho_{13} - i\Omega_1\rho_{23} + i\Omega_2\rho_{12} + i\Omega_3\rho_{14} \\
\frac{\partial \rho_{14}}{\partial t} &= (-i(\Delta_1 + \Delta_2 + \Delta_3) - \Gamma_4/2)\rho_{14} - i\Omega_1\rho_{24} + i\Omega_3\rho_{13} \\
\frac{\partial \rho_{24}}{\partial t} &= (-i(\Delta_2 + \Delta_3) - (\Gamma_2 + \Gamma_4)/2)\rho_{24} - i\Omega_1\rho_{14} - i\Omega_2\rho_{34} + i\Omega_3\rho_{23} \\
\frac{\partial \rho_{22}}{\partial t} &= -\Gamma_2\rho_{22} + i\Omega_1(\rho_{21} - \rho_{12}) + i\Omega_2(\rho_{23} - \rho_{32}) \\
\frac{\partial \rho_{33}}{\partial t} &= -\Gamma_3\rho_{33} + i\Omega_3(\rho_{34} - \rho_{43}) - i\Omega_2(\rho_{23} - \rho_{32}) \\
\frac{\partial \rho_{44}}{\partial t} &= -\Gamma_3\rho_{44} - i\Omega_3(\rho_{34} - \rho_{43})
\end{aligned} \tag{1}$$

where  $\Gamma_i$  are the decay constants of the levels  $i$  and  $\Delta_i = \omega_{i,i+1} - \omega_i$  are the laser detunings ( $\rho_{ij} = \rho_{ji}^*$  and  $\text{Tr}\rho = 1$ ). We study the steady state behaviour of the system for various values of the driving field strengths and detunings. In the general situation, we present the numerical solutions to the populations and coherences where the driving field strengths are treated up to all orders. The modification of the absorption profile of the ground state as well as the upper levels will be studied analytically by perturbatively solving for the density matrix elements in  $\Omega_2$  or  $\Omega_1$  as the case may be.

### 3 Weak middle transition coupling.

In the case when the transition  $2 \leftrightarrow 3$  is weakly coupled, i.e. when  $\Omega_2$  is very small compared to  $\Omega_1, \Omega_3$ , the equation of motion for the density matrix elements can be solved perturbatively in  $\Omega_2$ . The set of fifteen coupled equations decouples into three subsystems of equations which are solved independently to obtain analytical solutions. In fact, the density matrix elements given by the sets  $\{\rho_{11}, \rho_{22}, \rho_{12}, \rho_{21}\}, \{\rho_{33}, \rho_{34}, \rho_{43}, \rho_{44}\}$  and  $\{\rho_{23}, \rho_{13}, \rho_{14}, \rho_{24}\}$  form three subsystems. The zeroth and first order solutions for  $\rho_{ij}, i, j = 3, 4$  remain zero, while the coherences  $\{\rho_{23}, \rho_{24}, \rho_{13}, \rho_{14}\}$  are nonzero in the first order and are listed in the Appendix. The steady state second order solutions for  $\rho_{ij}$  are listed below:

$$\begin{aligned}
\rho_{22}^{(2)} &= (2\bar{\Gamma}_2\Omega_1^2(1 - \rho_{33}^{(2)} - \rho_{44}^{(2)}) - \Omega_2\text{Im}\rho_{23}^{(1)}(\Delta_1^2 + \bar{\Gamma}_2^2) + \\
&\quad 2\Omega_1\Omega_2(\Delta_1\text{Im}\rho_{13}^{(1)} + \bar{\Gamma}_2\text{Re}\rho_{13}^{(1)})/\mathcal{D}_1 \\
\rho_{12}^{(2)} &= -i(\bar{\Gamma}_2\Omega_1(i\Delta_1 - \bar{\Gamma}_2)(1 - \rho_{33}^{(2)} - \rho_{44}^{(2)}) + \bar{\Gamma}_2\Omega_2(i\Delta_1 - \bar{\Gamma}_2)\rho_{13}^{(1)} \\
&\quad + 2\Omega_1\Omega_2(i\Delta_1 - \bar{\Gamma}_2)\text{Im}\rho_{23}^{(1)} - 2\Omega_1^2\Omega_2(\rho_{13}^{(1)} - \rho_{31}^{(1)})/\mathcal{D}_1 \\
\rho_{33}^{(2)} &= (\bar{\Gamma}_4\Omega_2(\Delta_3^2 + (\bar{\Gamma}_3 + \bar{\Gamma}_4)^2) - 2\Omega_2\Omega_3^2(\bar{\Gamma}_3 + \bar{\Gamma}_4))\text{Im}\rho_{23}^{(1)} \\
&\quad + 2\Omega_2\Omega_3\bar{\Gamma}_4(\Delta_3\text{Im}\rho_{24}^{(1)} + (\bar{\Gamma}_3 + \bar{\Gamma}_4)\text{Re}\rho_{24}^{(1)})/\mathcal{D}_3 \\
\rho_{44}^{(2)} &= (2\Omega_2\Omega_3\bar{\Gamma}_3(\Delta_3\text{Im}\rho_{24}^{(1)} + (\bar{\Gamma}_3 + \bar{\Gamma}_4)\text{Re}\rho_{24}^{(1)}) + \Omega_2\Omega_3^2(\bar{\Gamma}_3 + \bar{\Gamma}_4)\text{Im}\rho_{23}^{(1)})/\mathcal{D}_3 \\
\rho_{34}^{(2)} &= i(2i\Omega_2\Omega_3^2(\bar{\Gamma}_4 + \bar{\Gamma}_3)\text{Im}\rho_{24}^{(1)} - \bar{\Gamma}_3\bar{\Gamma}_4\Omega_2(i\Delta_3 - \bar{\Gamma}_3 - \bar{\Gamma}_4)\rho_{24}^{(1)} \\
&\quad + \bar{\Gamma}_4\Omega_2\Omega_3(i\Delta_3 - (\bar{\Gamma}_3 + \bar{\Gamma}_4))\text{Im}\rho_{23}^{(1)})/\mathcal{D}_3 \tag{2}
\end{aligned}$$

where  $\mathcal{D}_1 = \bar{\Gamma}_2(\Delta_1^2 + \bar{\Gamma}_2^2 + 4\Omega_1^2)$  and  $\mathcal{D}_3 = 2\Omega_3^2(\bar{\Gamma}_3 + \bar{\Gamma}_4)^2 - \bar{\Gamma}_3\bar{\Gamma}_4(\Delta_3^2 + (\bar{\Gamma}_3 + \bar{\Gamma}_4)^2)$ . Here, for convenience we have relabeled  $\Gamma_i/2$  everywhere by  $\bar{\Gamma}_i$ . The second order steady state solutions for the set of coherences  $\{\rho_{23}, \rho_{13}, \rho_{24}, \rho_{14}\}$  are the same as the first order solutions given in the Appendix.

Note that, in the limit  $\Omega_2 \rightarrow 0$  and  $\Omega_3 \rightarrow 0$ , the solution for  $\rho_{12}$  and  $\rho_{22}$  are given by the zeroth order solutions which is the usual absorption and population of two-level system driven by a field of strength  $\Omega_1$ . There is very little modification in  $\rho_{12}$  and  $\rho_{22}$  due to the first order contribution. However the inclusion of the second order contribution introduces additional terms. Before investigating this further, let us look at the graphical illustration of the ground state absorption as a function of detuning which has been solved numerically for all orders in the driving field strengths. In Fig 2 the curve corresponding to (a) shows the absorption in the presence of only  $1 \leftrightarrow 2$  coupling, (b) corresponds to the absorption of the ground state (g.s.) in the presence of the  $1 \leftrightarrow 2$  as well as the  $2 \leftrightarrow 3$  couplings and (c) shows the modification of the g.s. absorption in the presence of the  $1 \leftrightarrow 2$  the first excited state coupling  $2 \leftrightarrow 3$  and the  $3 \leftrightarrow 4$  coupling. Here the small dip in the line center is not due to population trapping but due to the population transfer to the upper levels which is because of the inclusion of the upper most transition coupling. This becomes more clear by looking at equations (2) and (3) which will be discussed shortly. Let us look at

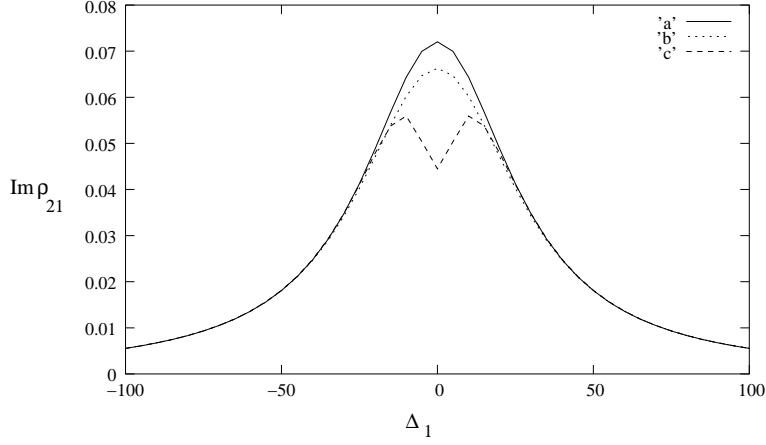


Figure 2:  $Im\rho_{21}$  as a function of the detuning  $\Delta_1$ . a)  $\Omega_1 = 20, \Omega_2 = \Omega_3 = 0$ , b)  $\Omega_1 = 20, \Omega_2 = 2, \Omega_3 = 0$ , c)  $\Omega_1 = 20, \Omega_2 = 2, \Omega_3 = 20$  and  $\Gamma_2 = 6, \Gamma_3 = \Gamma_4 = 1$ .

the variation of the populations of various levels as a function of  $\Omega_1$  and  $\Omega_3$  for very weak  $\Omega_2$ . Fig3-5 show the variation of populations w.r.t.  $\Omega_1$  and  $\Omega_3$  which have been obtained numerically. Note that  $\rho_{22}$  shows a dip in the absorption when  $\Omega_1 = \Omega_3$ . There is however a corresponding increase in the populations of the upper levels. Fig4 and Fig5 show a sharp increase in the absorption by level 3 and 4 respectively as  $\Omega_1$  approaches  $\Omega_3$  and shows a maxima for  $\Omega_1 = \Omega_3$  when  $\Omega_2 = 2$ .

One can explain this analytically by looking at the second order solutions. Consider the situation when all the detunings are zero and ignoring the contribution of the decay parameters  $O(\Gamma_i^2)$  i.e. assuming  $\Omega_{1,3} \gg \Gamma_{2,3,4}$  for  $\Delta_i = 0$ , the populations reduce to the simple form

$$\begin{aligned}
\rho_{22}^{(2)} &\approx \rho_{22}^{(0)} + \frac{\Omega_1^2 \Omega_2^2 \Omega_3^2 (\bar{\Gamma}_3 \rho_{22}^{(0)} - \Omega_1 Im\rho_{21}^{(0)})}{\Gamma_4 (\Omega_1^2 - \Omega_3^2) + \mathcal{G}} \\
Im\rho_{21}^{(2)} &\approx Im\rho_{21}^{(0)} + \frac{4\Omega_2^2 \Omega_3^2 \Omega_1 (\bar{\Gamma}_2 \rho_{22}^{(0)} (2\bar{\Gamma}_3 - \bar{\Gamma}_4) + Im\rho_{21}^{(0)} (-2\bar{\Gamma}_2 + \bar{\Gamma}_4) \Omega_1)}{\Gamma_4 (\Omega_1^2 - \Omega_3^2) + \mathcal{G}} \\
Im\rho_{34}^{(2)} &\approx \frac{\bar{\Gamma}_4 \Omega_2^2 \Omega_3 (-\rho_{22}^{(0)} \bar{\Gamma}_3 + \Omega_1 Im\rho_{21}^{(0)})}{2\Gamma_4 \Omega_3^2 (\Omega_1^2 - \Omega_3^2) + \mathcal{G}} \\
\rho_{33}^{(2)} &\approx \frac{\Omega_2^2 (2\Omega_3^2 (\bar{\Gamma}_4 - \bar{\Gamma}_3) \rho_{22}^{(0)} + 2\Omega_3^2 \Omega_1 Im\rho_{21}^{(0)})}{2\Gamma_4 \Omega_3^2 (\Omega_1^2 - \Omega_3^2) + \mathcal{G}} \\
\rho_{44}^{(2)} &\approx \frac{2\Omega_2^2 \Omega_3^2 (\bar{\Gamma}_3 \rho_{22}^{(0)} - \Omega_1 Im\rho_{21}^{(0)})}{2\Gamma_4 \Omega_3^2 (\Omega_1^2 - \Omega_3^2) + \mathcal{G}}
\end{aligned} \tag{3}$$

where  $\rho_{22}^{(0)} = 2\Omega_1^2 / (\bar{\Gamma}_2^2 + 4\Omega_1^2)$  and  $Im\rho_{21}^{(0)} = \bar{\Gamma}_2 \Omega_1 / (\bar{\Gamma}_2^2 + \Omega_1^2)$  for  $\Delta_1 = 0$  and  $\mathcal{G}$  includes terms of the  $O(\bar{\Gamma}_i^2)$ . It is obvious from these expressions that there is a resonance at  $\Omega_1 = \Omega_3$ . The populations  $\rho_{33}^{(2)}$  and  $\rho_{44}^{(2)}$  show a sharp rise as

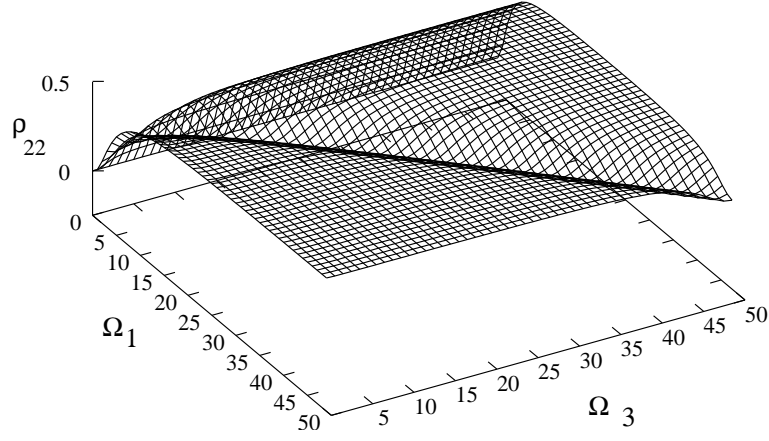


Figure 3:  $\rho_{22}$  as a function of the driving field strengths  $\Omega_1$  and  $\Omega_3$  with  $\Omega_2 = 2$  and  $\Gamma_2 = 6, \Gamma_3 = \Gamma_4 = 1$ . Occurrence of a minima for  $\Omega_1 = \Omega_3$ .

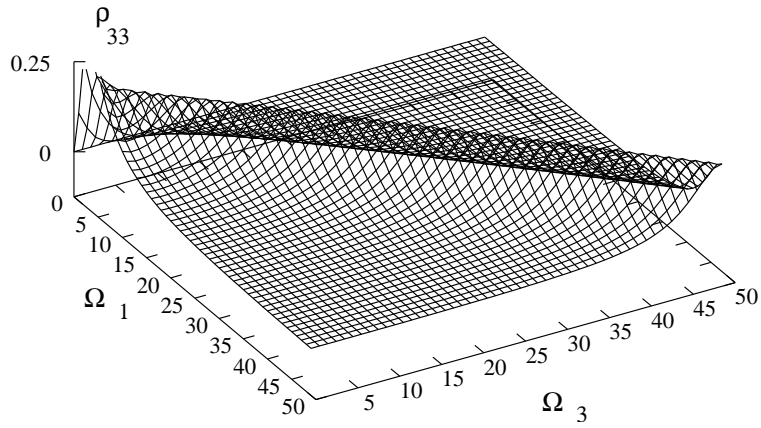


Figure 4:  $\rho_{33}$  as a function of the driving field strengths  $\Omega_1$  and  $\Omega_3$  with  $\Omega_2 = 2$ . Occurrence of a maxima for  $\Omega_1 = \Omega_3$ .

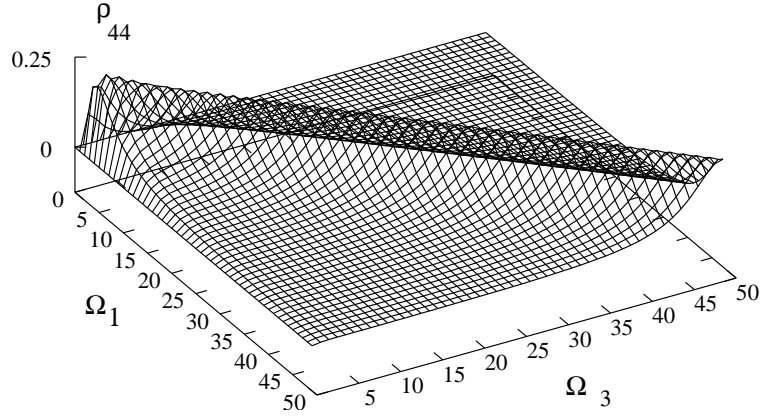


Figure 5:  $\rho_{44}$  as a function of the driving field strengths  $\Omega_1$  and  $\Omega_3$  with  $\Omega_2 = 2$  and  $\Gamma_2 = 6, \Gamma_3 = \Gamma_4 = 1$ . Occurrence of a maxima for  $\Omega_1 = \Omega_3$ .

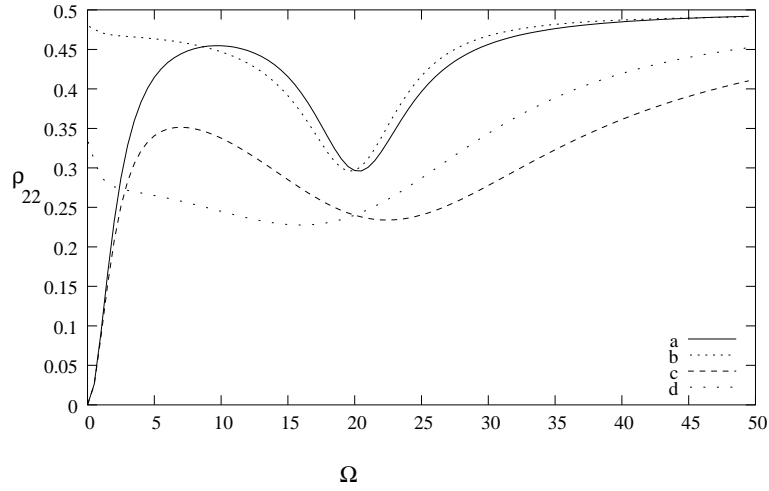


Figure 6:  $\rho_{22}$  as a function of the driving field strengths  $\Omega$  a)  $\Omega_2 = 2, \Omega_1 = 20, \Omega = \Omega_3$  b)  $\Omega_3 = 20, \Omega_2 = 2, \Omega = \Omega_1$  c)  $\Omega_2 = 8, \Omega_1 = 20, \Omega = \Omega_3$  d)  $\Omega_3 = 20, \Omega_2 = 8, \Omega = \Omega_1$ . Here,  $\Gamma_2 = 6, \Gamma_3 = \Gamma_4 = 1$ .

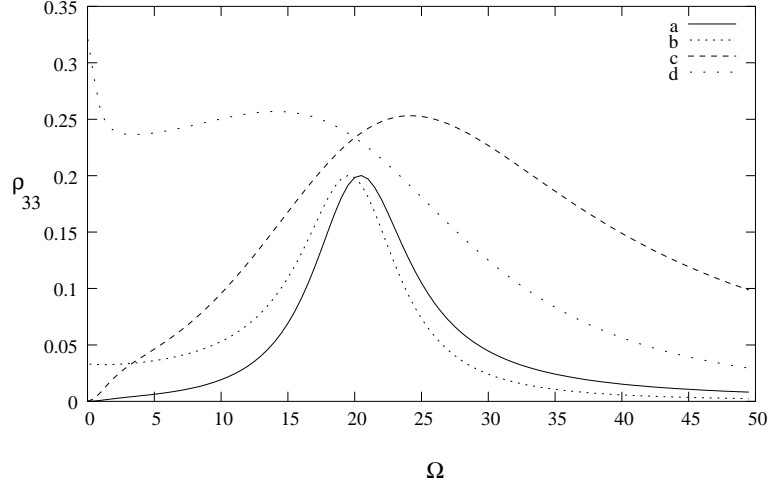


Figure 7:  $\rho_{33}$  as a function of the driving field strengths  $\Omega$  a)  $\Omega_2 = 2, \Omega_1 = 20, \Omega = \Omega_3$  b)  $\Omega_3 = 20, \Omega_2 = 2, \Omega = \Omega_1$  c)  $\Omega_2 = 8, \Omega_1 = 20, \Omega = \Omega_3$  d)  $\Omega_3 = 20, \Omega_2 = 8, \Omega = \Omega_1$ . Here,  $\Gamma_2 = 6, \Gamma_3 = \Gamma_4 = 1$ .

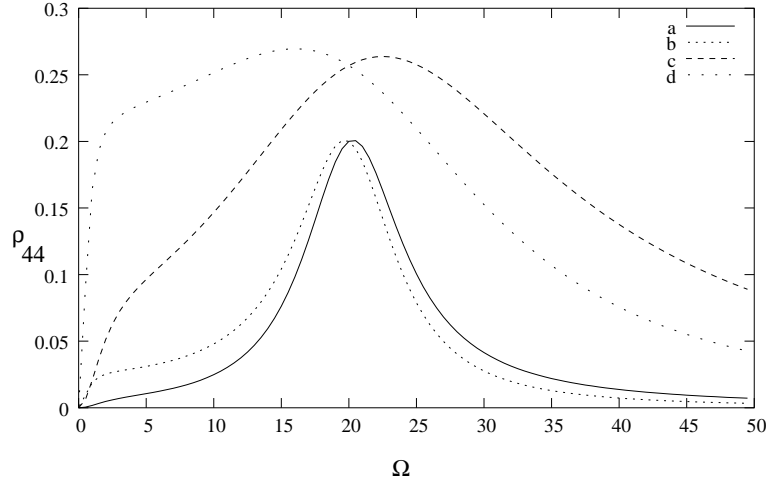


Figure 8:  $\rho_{44}$  as a function of the driving field strengths  $\Omega_1$ . a)  $\Omega_2 = 2, \Omega_1 = 20, \Omega = \Omega_3$  b)  $\Omega_3 = 20, \Omega_2 = 2, \Omega = \Omega_1$  c)  $\Omega_2 = 8, \Omega_1 = 20, \Omega = \Omega_3$  d)  $\Omega_3 = 20, \Omega_2 = 8, \Omega = \Omega_1$ . Here,  $\Gamma_2 = 6, \Gamma_3 = \Gamma_4 = 1$ .



$\Omega_1 \rightarrow \Omega_3$  since the numerator is positive. Thus to populate the levels 3 and 4 maximally when the middle level coupling is weak, it is sufficient to match the requirement  $\Omega_1 = \Omega_3$ . The absorption profile  $Im\rho_{34}^{(2)}$  also shows a similar trend. While the second term in  $\rho_{22}^{(2)}$  and  $\rho_{21}^{(2)}$  are negative and the role of the resonance in the denominator is to introduce a minima when  $\Omega_1 = \Omega_3$ . Thus the role of the second order term in this case, is to introduce a dip in the line center in an otherwise two-level absorption profile and hence a depletion in the population of level 2. As one increases  $\Omega_2$  this perturbative expansion is no longer valid. Moreover, the numerical calculations upto all orders in  $\Omega_2$  reveal the fact that the resonance condition becomes weaker and the sharp features vanish. This is demonstrated graphically in Fig6-8.

Thus, in a four-level system with middle transition coupling very weak, the condition for maximally populating the upper levels is to satisfy this resonance condition. The population transfer to higher levels occurs at the cost of depletion of population in the second level. This modification is mediated by the contribution of the coherences, which at three photon resonance are given by  $\rho_{23}^{(1)} \approx \Omega_2 Im\rho_{21}^{(0)}/\mathcal{G}_0$ ,  $\rho_{13}^{(1)} \approx \Omega_1\Omega_2\rho_{22}^{(0)}/\mathcal{G}_0$ ,  $\rho_{24}^{(1)} \approx \Omega_2\Omega_3\rho_{22}^{(0)}/\mathcal{G}_0$  where  $\mathcal{G}_0 = \bar{\Gamma}_4(\Omega_1^2 - \Omega_3^2)$ .

## 4 Strong middle transition coupling

I next consider the case when the  $2 \rightarrow 3$  transition is strongly coupled i.e.,  $\Omega_2 \gg \Omega_1, \Omega_3$ . Treating  $\Omega_1$  perturbatively, the first order absorption of the ground state takes the simple form [2]

$$Im\rho_{21}^{(1)} = \frac{L_{12} + \Omega_3^2/L_{123}\Omega_1}{(\Omega_2^2 + L_1L_{12} + \Omega_3^2L_1/L_{123})} \quad (4)$$

where  $L_1 = (-i\Delta_1 - \Gamma_2/2)$ ,  $L_{12} = (-i(\Delta_2 + \Delta_1) - \Gamma_3/2)$  and  $L_{123} = (-i(\Delta_1 + \Delta_2 + \Delta_3) - \Gamma_4/2)$ . We now look at some simple situations, for example when  $\Omega_2 \rightarrow 0$ ,  $\Omega_3 \rightarrow 0$ , the absorption becomes proportional to  $\Gamma_2\Omega_1/(\Delta_1^2 + \Gamma_2^2)$  which is the ground state absorption for a weak excitation and observe that the width is proportional to  $\Gamma_2$ . Next, consider only  $\Omega_3 \rightarrow 0$ . The absorption is now given by

$$Im\rho_{21} = \frac{\Omega_1(\Delta_1^2\bar{\Gamma}_2 + \bar{\Gamma}_3(\bar{\Gamma}_3\bar{\Gamma}_2 + \Omega_2^2))}{\Delta_1^4 + \Delta_1^2(\bar{\Gamma}_2^2 + \bar{\Gamma}_3^2 - 2\Omega_2^2) + (\bar{\Gamma}_2\bar{\Gamma}_3 + \Omega_2^2)^2} \quad (5)$$

where  $\Delta_2$  is assumed to be zero. The denominator is quadratic in  $\Delta_1^2$  and hence has two peaks corresponding to the usual Autler-Townes doublet. The width of this EIT window is proportional to  $\sqrt{(\bar{\Gamma}_2^2 + \bar{\Gamma}_3^2 - 2\Omega_2^2)^2 - 4(\bar{\Gamma}_2\bar{\Gamma}_3 + \Omega_2^2)}$ . The absorption for  $\Delta_1 = 0$  (at the line center) is proportional to  $\Omega_1\bar{\Gamma}_3/(\bar{\Gamma}_2\bar{\Gamma}_3 + \Omega_2^2)$  which is negligible since it is of the order  $\Omega_1/\Omega_2^2$ . The absorption in the presence of the third driving field for  $\Delta_2 = 0$ ,  $\Delta_3 = 0$  takes the simplified form

$$Im\rho_{21}^{(1)} = \frac{\Omega_1(\Delta_1^2(\Delta_1^2\bar{\Gamma}_2 + \bar{\Gamma}_2(\bar{\Gamma}_3^2 + \bar{\Gamma}_4^2) + \bar{\Gamma}_3\Omega_2^2 - 2\bar{\Gamma}_2\Omega_3^2) + T_1)}{\Delta_1^2(\Delta_1^2 - \Gamma_p - \Omega_2^2 - \Omega_3^2)^2 + (\Delta_1^2\Gamma_s - \bar{\Gamma}_2\bar{\Gamma}_3\bar{\Gamma}_4 - \bar{\Gamma}_4\Omega_2^2 - \bar{\Gamma}_2\Omega_3^2)^2} \quad (6)$$

where  $\Gamma_s = \bar{\Gamma}_2 + \bar{\Gamma}_3 + \bar{\Gamma}_4$ ,  $\Gamma_p = \bar{\Gamma}_2\bar{\Gamma}_3 + \bar{\Gamma}_3\bar{\Gamma}_4 + \bar{\Gamma}_4\bar{\Gamma}_2$  and  $T_1 = \bar{\Gamma}_2\bar{\Gamma}_3^2\bar{\Gamma}_4^2 + \bar{\Gamma}_3\bar{\Gamma}_4^2\Omega_2^2 + 2\bar{\Gamma}_2\bar{\Gamma}_3\bar{\Gamma}_4\Omega_3^2 + \bar{\Gamma}_4\Omega_3^2\Omega_2^2 + \bar{\Gamma}_2\Omega_3^4$ . The denominator is a cubic equation in  $\Delta_1^2$  with the three roots corresponding to the three absorption peaks, two of them correspond to the usual Autler-Townes doublet and the absorption at the line center is due to the three photon interaction and is proportional to  $\Omega_1\Omega_3^2/(\bar{\Gamma}_4\Omega_2^2 + \bar{\Gamma}_2\Omega_3^2)$  which occurs when all the detunings are zero. This three peaked absorption in four level systems has been observed earlier and has been frequently referred to as the splitting of the EIT window. While the role of the strong  $2 \leftrightarrow 3$  coupling was to introduce transparency at the line center, the role of the  $3 \leftrightarrow 4$  coupling is to induce a narrow absorption at the line center within the EIT window. Thus the two photon absorption was responsible for the coherence  $\rho_{31}$  which in turn lead to non-absorption while, the three photon absorption which introduced a coherence between levels 1 and 4 ( $\rho_{41}$ ) which in turn induced this sharp absorption feature. Thus there is a contrast in the nature of the quantum interference in the case of two and three photon interaction.

On the other hand consider the case when the detuning  $\Delta_3$  is nonzero. Let  $\Delta_1 = 0, \Delta_2 = 0$ , the absorption now reduces to

$$Im\rho_{21}^{(1)} = \frac{\Omega_1(\Delta_3^2\bar{\Gamma}_3(\bar{\Gamma}_2\bar{\Gamma}_3 + \Omega_2^2) + (\bar{\Gamma}_3\bar{\Gamma}_4 + \Omega_3^2)(\bar{\Gamma}_4\Omega_2^2 + \bar{\Gamma}_2(\bar{\Gamma}_3\bar{\Gamma}_4 + \Omega_3^2)))}{\Delta_3^2(\bar{\Gamma}_2\bar{\Gamma}_3 + \Omega_2^2)^2 + (\bar{\Gamma}_4\Omega_2^2 + \bar{\Gamma}_2(\bar{\Gamma}_3\bar{\Gamma}_4 + \Omega_3^2))^2} \quad (7)$$

This is a Lorentzian with width proportional to  $\bar{\Gamma}_2\Omega_3^2/\Omega_2^2$ . This implies that the line width can be subnatural ( $< \Gamma_2$ ) for  $\Omega_3 < \Omega_2$ . Notice the novel feature here which is the absence of the Autler-Townes doublet unlike the case when only  $\Delta_1$  was nonzero. Thus, we now have obtained a powerful technique for filtering the Autler-Townes doublet and retaining only the narrow absorption at the line center in addition to gaining control over the linewidth. This could prove to be a useful technique in high resolution spectroscopy.

A numerical illustration of these novel features is presented in Fig 9 where the steady state solutions are obtained for all orders in the driving field strengths. Figure 9 clearly shows the difference in the behaviour depending on the strength of the middle transition coupling. a) corresponds to weak  $\Omega_2$  while b) corresponds to strong  $\Omega_2$ . Fig 9A-b shows the three peaked absorption while Fig9B-b shows the elimination of the Autler-Townes doublet by detuning the driving field coupling 3-4 transition as predicted by the perturbative calculations. Likewise for small  $\Omega_2$ , only the narrow absorption dip at the line center is seen by detuning  $\Delta_3$ (Fig 9A-a and Fig9B-a). Again,  $Im\rho_{32}$  for small  $\Omega_2$  is very strong (Fig9C-a) as the perturbation calculation indicate (section III) and this absorption is not very significant for large  $\Omega_2$  since the resonance condition weakens and the contribution of higher order terms in  $\Omega_2$  dominate. Lastly, the absorption profile of the uppermost transition does not seem to vary much with either of the detunings  $\Delta_1$  or  $\Delta_3$  (Fig9-Eb, Fig9F-b). This is very much similar to the narrow g.s. absorption at the line center. Further, both the absorption of the g.s.(line center) and the upper most transition  $Im\rho_{43}$  are unaffected by the detunings  $\Delta_1/\Delta_3$  since they occur at exact three photon resonance. One would expect this absorption feature also to be Doppler-free like the g.s. absorption [2].

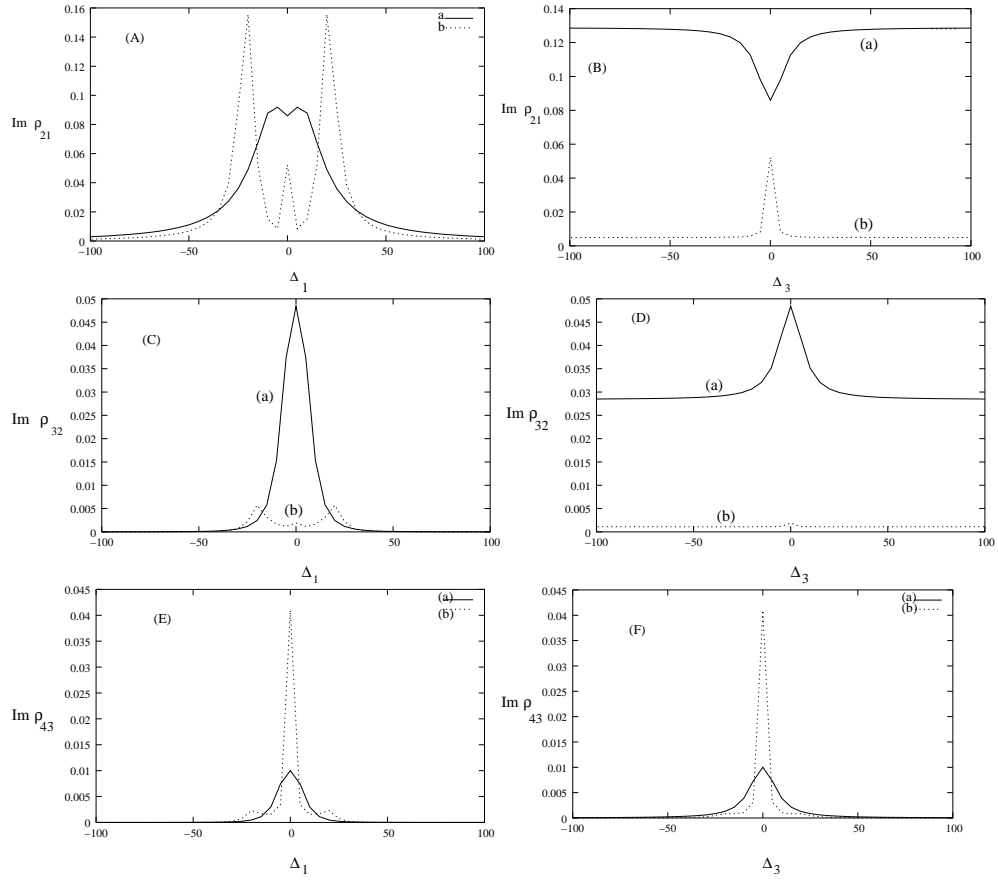


Figure 9: The variation of absorption for (a)  $\Omega_2 = 2, \Omega_1 = \Omega_3 = 20$  and (b)  $\Omega_2 = 20, \Omega_1 = \Omega_3 = 4$ . A)  $\text{Im} \rho_{21}$  with  $\Delta_1$  B)  $\text{Im} \rho_{21}$  with  $\Delta_3$ . C)  $\text{Im} \rho_{32}$  with  $\Delta_1$  D)  $\text{Im} \rho_{32}$  with  $\Delta_3$  E)  $\text{Im} \rho_{43}$  with  $\Delta_1$  F)  $\text{Im} \rho_{43}$  with  $\Delta_3$  with the  $\Gamma_i, i = 2, 4$  the same as in the previous figures.

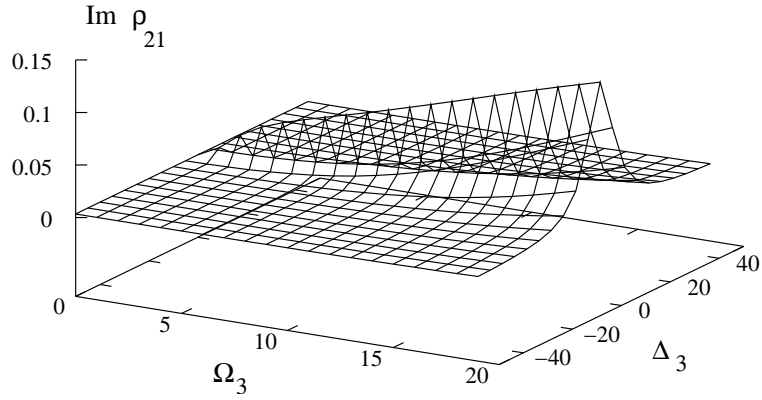


Figure 10:  $Im\rho_{21}$  as a function of  $\Omega_3$  and  $\Delta_3$  with parameter values  $\Delta_1 = \Delta_2 = 0$   $\Omega_1 = 4, \Omega_2 = 20$  and  $\Gamma_i, i = 2, 4$  the same as the previous figures.

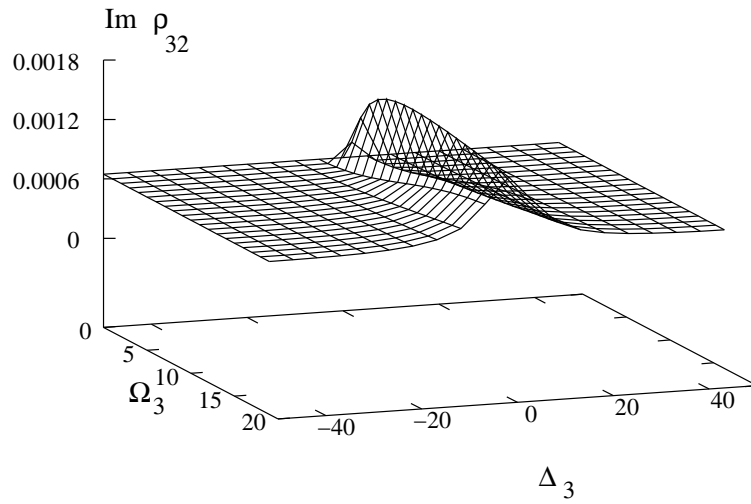


Figure 11:  $Im\rho_{32}$  as a function of  $\Omega_3$  and  $\Delta_3$  with  $\Delta_1 = \Delta_2 = 0$  and the rest of the parameters the same as in the previous figure.

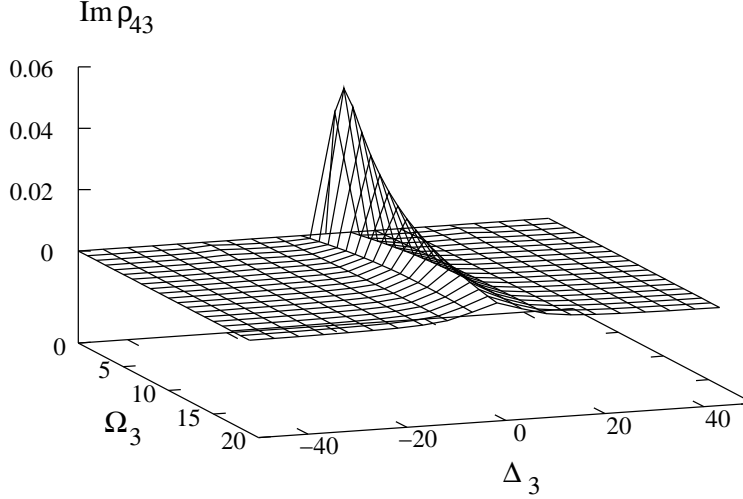


Figure 12:  $Im\rho_{43}$  as a function of  $\Omega_3$  and  $\Delta_3$  for parameter values the same as in previous figure.

Next the variation of the absorption of the g.s.,  $Im\rho_{21}$ , the first excited state  $Im\rho_{32}$  and the second excited state  $Im\rho_{43}$  with the driving field strength  $\Omega_3$  and the detuning  $\Delta_3$  are numerically illustrated in Fig10-12. The purpose here, is to demonstrate the three photon effect. While the ground state absorption increases with  $\Omega_3$ , the middle and the upper transition absorptions rise sharply for small  $\Omega_3$  and fall rapidly to zero. All the absorption occurs only for  $\Delta_3 = 0$ . The variation with  $\Delta_2$  shows lot more structure and will be more appropriate to present it else where.

To summarise, it is shown that by satisfying the resonance condition  $\Omega_1 = \Omega_3$  one can maximally populate the upper levels at the cost of depleting the population of level 2 (for small  $\Omega_2$ ). In the case of large  $\Omega_2$  it is shown that one can get narrow absorption features at the line center by filtering of the Autler-Townes doublet. One also has a control over the line-width by controlling  $\Omega_2$  and  $\Omega_3$ . The qualitative features predicted by perturbative calculations seem to agree very well with the numerical results.

## 5 Appendix

The zeroth order equation in  $\Omega_2$  are given by

$$\begin{aligned} \frac{\partial \rho_{12}^{(0)}}{\partial t} &= (-i\Delta_1 - \Gamma_2/2)\rho_{12}^{(0)} - i\Omega_1(\rho_{22}^{(0)} - \rho_{11}^{(0)}) \\ \frac{\partial \rho_{22}^{(0)}}{\partial t} &= -\Gamma_2\rho_{22}^{(0)} + i\Omega_1(\rho_{21}^{(0)} - \rho_{12}^{(0)}) \end{aligned}$$

$$\frac{\partial \rho_{21}^{(0)}}{\partial t} = (i\Delta_1 - \Gamma_2/2)\rho_{21}^{(0)} + i\Omega_1(\rho_{22}^{(0)} - \rho_{11}^{(0)})$$

the rest of the density matrix elements are zero (steady state). The first order equation do not contribute to the solutions of  $\rho_{ij}$ ,  $i, j = 1, 2$ . The density matrix elements  $\rho_{ij}$ ,  $i, j = 3, 4$  remain zero. Hence we furnish below the first order equations for the coherences only.

$$\begin{aligned} \frac{\partial \rho_{23}^{(1)}}{\partial t} &= (-i\Delta_2 - (\Gamma_2 + \Gamma_3)/2)\rho_{23} - i\Omega_1\rho_{13}^{(1)} - i\Omega_2(-\rho_{22}^{(0)}) + i\Omega_3\rho_{24}^{(1)} \\ \frac{\partial \rho_{13}^{(1)}}{\partial t} &= (-i(\Delta_1 + \Delta_2) - \Gamma_3/2)\rho_{13}^{(1)} - i\Omega_1\rho_{23}^{(1)} + i\Omega_2\rho_{12}^{(0)} + i\Omega_3\rho_{14}^{(1)} \\ \frac{\partial \rho_{14}^{(1)}}{\partial t} &= (-i(\Delta_1 + \Delta_2 + \Delta_3) - \Gamma_4/2)\rho_{14}^{(1)} - i\Omega_1\rho_{24}^{(1)} + i\Omega_3\rho_{13}^{(1)} \\ \frac{\partial \rho_{24}^{(1)}}{\partial t} &= (-i(\Delta_2 + \Delta_3) - (\Gamma_2 + \Gamma_4)/2)\rho_{24}^{(1)} - i\Omega_1\rho_{14}^{(1)} + i\Omega_3\rho_{23}^{(1)} \end{aligned} \quad (8)$$

the first order steady state solutions of these equations are given by

$$\begin{aligned} \rho_{23}^{(1)} &= \frac{\Omega_2(\Omega_1\rho_{12}^{(0)}(\Omega_1^2 - \Omega_3^2 + L_{123}L_{23}) + i\rho_{22}^{(0)}(L_{12}L_{23}L_{123} + L_{12}\Omega_1^2 + L_{23}\Omega_3^2))/\mathcal{D}_2}{\Omega_1\rho_{22}^{(0)}(\Omega_1^2 - \Omega_3^2 + L_{123}L_{23})/\mathcal{D}_2} \\ \rho_{13}^{(1)} &= \frac{\Omega_2(i\rho_{12}^{(1)}(L_{123}L_2L_{23} + L_2\Omega_1^2 + L_{123}\Omega_3^2) - \Omega_1\rho_{22}^{(0)}(\Omega_1^2 - \Omega_3^2 + L_{123}L_{23}))/\mathcal{D}_2}{\Omega_1\rho_{22}^{(0)}(\Omega_1^2 - \Omega_3^2 + L_{123}L_{23})/\mathcal{D}_2} \\ \rho_{24}^{(1)} &= \frac{-\Omega_2\Omega_3(\rho_{22}^{(0)}(L_{12}L_{123} - \Omega_1^2 + \Omega_3^2) + i\Omega_1\rho_{12}^{(0)}(L_{123} + L_2))/\mathcal{D}_2}{\Omega_1\rho_{22}^{(0)}(\Omega_1^2 - \Omega_3^2 + L_{123}L_{23})/\mathcal{D}_2} \\ \rho_{14}^{(1)} &= \frac{\Omega_2\Omega_3(\rho_{22}^{(0)}(\Omega_1^2 - \Omega_3^2 - L_{12}L_{123}) + i\Omega_1\rho_{12}^{(0)}(L_{123} + L_2))/\mathcal{D}_2}{\Omega_1\rho_{22}^{(0)}(\Omega_1^2 - \Omega_3^2 + L_{123}L_{23})/\mathcal{D}_2} \end{aligned}$$

where  $\mathcal{D}_2 = ((\Omega_1^2 - \Omega_3^2)^2 + \Omega_1^2(L_{123}L_{23} + L_{12}L_2) + \Omega_3^2(L_{12}L_{123} + L_2L_{23}) + L_{12}L_{23}L_{123}L_{23})$  and  $L_2 = (-i\Delta_2 - (\Gamma_2 + \Gamma_3)/2)$ ,  $L_{23} = (-i(\Delta_2 + \Delta_3) - (\Gamma_2 + \Gamma_4)/2)$  while  $L_{12}$  and  $L_{123}$  are given in the text. The second order equations are given by

$$\begin{aligned} \frac{\partial \rho_{12}^{(2)}}{\partial t} &= (-i\Delta_1 - \Gamma_2/2)\rho_{12}^{(2)} - i\Omega_1(\rho_{22}^{(2)} - \rho_{11}^{(2)}) + i\Omega_2\rho_{13}^{(1)} \\ \frac{\partial \rho_{22}^{(2)}}{\partial t} &= -\Gamma_2\rho_{22}^{(2)} + i\Omega_1(\rho_{21}^{(2)} - \rho_{12}^{(2)}) + i\Omega_2(\rho_{23}^{(1)} - \rho_{32}^{(1)}) \\ \frac{\partial \rho_{34}^{(2)}}{\partial t} &= (-i\Delta_3 - (\Gamma_3 + \Gamma_4)/2)\rho_{34}^{(2)} - i\Omega_2\rho_{24}^{(1)} - i\Omega_3(\rho_{44}^{(2)} - \rho_{33}^{(2)}) \\ \frac{\partial \rho_{33}^{(2)}}{\partial t} &= -\Gamma_3\rho_{33}^{(2)} + i\Omega_3(\rho_{34}^{(2)} - \rho_{43}^{(2)}) - i\Omega_2(\rho_{23}^{(1)} - \rho_{32}^{(1)}) \\ \frac{\partial \rho_{44}^{(2)}}{\partial t} &= -\Gamma_3\rho_{44}^{(2)} - i\Omega_3(\rho_{34}^{(2)} - \rho_{43}^{(2)}) \end{aligned}$$

So far, we dealt with equations where  $\Omega_2$  was treated perturbatively. I furnish below the relevant first order equations where  $\Omega_1$  is treated perturbatively,

$$\begin{aligned}\frac{\partial \rho_{12}^{(1)}}{\partial t} &= (-i\Delta_1 - \Gamma_2/2)\rho_{12}^{(1)} - i\Omega_1 + i\Omega_2\rho_{13}^{(1)} \\ \frac{\partial \rho_{13}^{(1)}}{\partial t} &= (-i(\Delta_1 + \Delta_2) - \Gamma_3/2)\rho_{13}^{(1)} + i\Omega_2\rho_{12}^{(1)} + i\Omega_3\rho_{14}^{(1)} \\ \frac{\partial \rho_{14}^{(1)}}{\partial t} &= (-i(\Delta_1 + \Delta_2 + \Delta_3) - \Gamma_4/2)\rho_{14}^{(1)} + i\Omega_3\rho_{13}^{(1)}\end{aligned}$$

## Acknowledgments

I thank Professor G S Agarwal for useful discussions. I wish to thank the Department of Science and Technology for Financial support under the WOS-A scheme.

## References

## References

- [1] see for eg. *Quantum Optics* by M O Scully and M S Zubairy, Cambridge Univ. Press (1997).
- [2] S N Sandhya and K K Sharma, Phys.Rev. **A 55** 2155 (1996).
- [3] Yelin et al, Phys. Rev. **A 68** 063801(2003); M D Lukin et al, Phys. Rev.**A 60** 3225 (1999).
- [4] C Y Ye et al, Phys. Rev.**A 65** 043805 (2002)
- [5] B S Ham and P R Hemmer, Phys. Rev. Lett. **84** 4080 (2000).
- [6] Harris and Yamomoto, Phys.Rev. Lett.**81** 3611 (1998).
- [7] M Yan, E G Rickey and Y Zhu,Phys. Rev.**A 64** 041801(R) (2001).
- [8] G S Agarwal and Harshawardhan, Phys.Rev.Lett. **77** 1039(1996).
- [9] M Yan, E G Rickey and Y Zhu, Phys.Rev.**A 64** 013412 (2001).
- [10] Yang et al, Phys.Rev.**72** 053801 (2005).
- [11] C Wei et al, Phys. Rev. A 58 2310 (1998); S R de Echaniz et al, Phys. Rev. **A 64** 013812 (2001).
- [12] S N Sandhya, Opt.Comm. **217** 291 (2003).